AIP Advances

Fabrication of externally wetted emitter for ionic liquid electrospray thruster by low-speed wire cutting combined with electrochemical etching

Cite as: AIP Advances **11**, 115023 (2021); https://doi.org/10.1063/5.0072630
Submitted: 23 September 2021 • Accepted: 30 October 2021 • Published Online: 16 November 2021

Senwen Xue, Li Duan and Qi Kang

View Online Export Citation CrossMark

ARTICLES YOU MAY BE INTERESTED IN

The role of secondary species emission in vacuum facility effects for electrospray thrusters
Journal of Applied Physics **130**, 143301 (2021); https://doi.org/10.1063/5.0063476

Multi-scale modeling of ionic electrospray emission
Journal of Applied Physics **131**, 014902 (2022); https://doi.org/10.1063/5.0071483

Taking internally wetted capillary electrospray emitters to the sub-ten-micrometer scale with 3D microlithography
AIP Advances **11**, 105315 (2021); https://doi.org/10.1063/5.0066619

AIP Publishing

© 2021 Author(s).

Fabrication of externally wetted emitter for ionic liquid electrospray thruster by low-speed wire cutting combined with electrochemical etching

Cite as: AIP Advances 11, 115023 (2021); doi: 10.1063/5.0072630
Submitted: 23 September 2021 • Accepted: 30 October 2021 •
Published Online: 16 November 2021

View Online Export Citation CrossMark

Senwen Xue, Li Duan, and Qi Kang[a)]

AFFILIATIONS

Key Laboratory of Microgravity, Institute of Mechanics, Chinese Academy of Sciences, Beijing 100190, People's Republic of China and School of Engineering Sciences, University of Chinese Academy of Sciences, Beijing 100049, People's Republic of China

[a)]Author to whom correspondence should be addressed: kq@imech.ac.cn

ABSTRACT

The micro-newton thrust generated by an ionic liquid electrospray thruster (ILET) can be used for drag-free control, attitude precise control, networking, and formation flight of micro-nano-satellites or spacecraft. Fabrication of high-quality emitters is one of the key technologies for the application of ILETs. A new method for fabricating externally wetted emitters is presented in this article. This method uses low-speed wire cutting (LSWC) combined with electrochemical etching, and the externally wetted emitter is fabricated in three steps. First, the tungsten cuboid is shaped by LSWC to get the geometry of the emitter. Second, the emitter is cleaned by superacid to remove the oxide layer that critically prevents the ionic liquid from wetting the emitter. Finally, microchannels are etched on the emitter surface by electrochemical etching. The tungsten emitter fabricated by the above-mentioned steps can obtain excellent wettability, and its microchannel can reduce the contact angle between the wall and the ionic liquid and enhance the capillary force that promotes the ionic liquid to climb along the emitter. The ionic liquid is spread into a uniform liquid film on the emitter surface to ensure a stable and continuous flow supply so that the thruster can work in pure ionic emission mode for a long time with low noise, high resolution, and a high thrust power ratio. The quantitative and qualitative analysis of all elements before and after the pickling emitter proves the feasibility of removing the oxide layer. The morphology features of the emitter are measured and observed using a metallographic microscope and profilometer, including the microchannel structure and its size and tip size and the thickness of the liquid film. Through repeated observation and evaluation, the etching parameters are recorded, including the amplitude and frequency of AC voltage, the etching time, the depth of emitter immersion in the solution, and the concentration of NaOH solution. In order to compare the performance of an externally wetted emitter and a porous emitter, the same process is used to fabricate two kinds of emitters. The conclusions on beam current, the resolution and noise of beam current, ignition reliability, and emission time are summarized during the emission testing. The emission tests indicate that the externally wetted emitter exhibits outstanding performance, which depends on its better wettability and the fact that the microchannels are not easily blocked by the products of electrochemical reaction.

© 2021 Author(s). All article content, except where otherwise noted, is licensed under a Creative Commons Attribution (CC BY) license (http://creativecommons.org/licenses/by/4.0/). https://doi.org/10.1063/5.0072630

I. INTRODUCTION

Ionic liquid ion sources (ILISs) have been investigated vigorously in the last few decades.[1] ILISs use ionic liquids that are a kind of molten salt at room temperature to emit evaporated ions in a strong electrostatic field. They provide high luminosity ion beams for an number of important applications in microfabrication, focused ion beam systems, material deposition, material analysis, lithography, and surface modification and have been proposed as space thrusters for diverse types of spacecraft because of their unique characteristics such as small volume, low power consumption, equivalently high currents, shallow implantation depths, low implantation damage, easy negative ion beam extraction, and numerous molecular combinations.[2–9] Compared with a liquid metal ion source (LMIS), an ILIS has a lower emission voltage threshold without a heating device.

The ionic liquid electrospray thruster (ILET) is one of the most important applications of an ILIS. An ILET can contribute to drag-free control, attitude precise control, networking, and

formation flight of micro-nano-satellites or spacecraft. ILETs can be divided into three types according to the emitter wetting mode: externally wetted,[5,6,10–12] capillary,[13–16] and porous.[17–22] The advantages of a capillary emitter are embodied in propellant management and transportation. The capillary emitter can adjust the thruster performance by changing the flow rate. The method commonly used is differential pressure, which requires a high-pressure storage unit and complex piping and valves to keep the flow rate below 10 nl/s and also adds complexity to the entire propulsion system. Therefore, the capillary emitter is not suitable for micro-nano-satellites with very limited volume and mass. However, a large range or high precision thrust adjustment can be achieved by changing the flow rate for medium-sized satellites over 100 kg. It is a potential application direction of the capillary emitter. For instance, the American Busek company has developed a CMNT (Colloid Micro-Newton Thruster) for ST7-DRS (Space Technology 7 Disturbance Reduction System) and LISA (Laser Interferometer Space Antenna) missions.[23–26] Most remarkable of all the types, the externally wetted ILET is becoming more prevalent since the ionic liquid can be passively fed through the microchannels by capillary force without any micropumps, microvalves, or pipelines. This is especially attractive for space propulsion applications in which compact structure and light weight are expected.

The emitter is the essential component of the ILET. In order to obtain sufficient electric field intensity at the vicinity of the emitter tip that allows the ion or ion cluster to break through the energy barrier and escape from the phase interface to form effective beam current, the emitter is usually designed in sharp shapes, such as a needle, V-blade, or pyramid. The quality of the emitter directly determines the performance of the ILET. Foremost, the curvature diameter of the emitter tip should be etched to less than 10 μm, which can make the thruster easier to operate in pure ionic emission mode for a long time and lower the emission voltage threshold. In addition to this, the numerous microchannels etched on the emitter surface should be wide and deep enough to ensure adequate liquid supply even if a few are blocked by the products of electrochemical reactions after a long-time emission under bias voltage.

A large number of scholars have made tremendous efforts in the fabrication of externally wetted emitters. Table I lists the materials and technologies used to fabricate externally wetted emitters that are representative in lots of literature studies. A survey on the fabricating technologies for externally wetted emitters since 2000 reveals that there exist two main methods. First, the micro-electromechanical system (MEMS) is suitable for the miniaturization of the electrospray thruster array, which can etch the emitter structure with a large depth–width ratio on a silicon chip and ensure the array has good consistency. However, the MEMS requires professional operating skills and expensive facilities, which are very unfriendly to laboratories with a weak foundation. The high integration of the MEMS means that large thrust densities (μN/mm^2) can be achieved but are limited by the choice of emitter materials. Second, electrochemically etched tungsten wires are widely used in the field of scanning tunneling microscopy[36–40] and various ion sources.[33,41] The tip size can be controlled to within 10 μm, which fully satisfies the needs of electrospray thrusters. The only disadvantage is that the electrospray thruster array fabricated by electrochemical etching is not highly integrated compared to the MEMS. This is due to the fact that the size of an electrochemically etched single unit is usually on the millimeter scale rather than the nanometer to micrometer scale of the MEMS. An oversized emitter requires a certain roughness to obtain excellent wettability. A rough emitter has many grooves on the surface that determine the resistance for the fluid to move toward the tip. Under DC voltage, the immersed part of the tungsten wire in the electrolyte drops off due to reaction, and a sharp tip with the smooth surface is formed. Surface roughening is implemented by the electrochemical etching under AC voltages or dipping into a saturated solution of 1 mol NaOH and $K_3Fe(CN)_6$ at 60 °C combined annealing.[10,33]

To sum up, it is feasible to obtain a single rough and qualified emitter simply by electrochemically etching tungsten wire. If the electrospray thruster array is fabricated in the same way, the emitters will show very poor consistency and wettability. In order to solve these problems, a new technique for fabricating an externally wetted emitter is proposed in the article, which is described as low-speed wire cutting (LSWC) combined with electrochemical etching. Low-speed wire cutting is a traditional high precision machining technology that can fabricate designed geometry and a uniform array. Next, the tip is sharped and the emitter is roughened by electrochemical etching under DC voltage or AC voltage, respectively. After the geometry of the emitter is fixed, the size of the tip and the roughness of the emitter can be controlled by adjusting the amplitude of the etching voltage, the frequency of the AC voltage, the etching time, and the concentration of the electrolyte. The externally wetted emitter fabricated by the above-mentioned technology is assembled as a hybrid structure that can construct a stable meniscus to continuously wet the emitter.[42] The fabricating parameters are

TABLE I. The externally wetted emitter materials and fabrication technologies in the literature.

Researchers	Material	Geometry	Fabrication technology
Lozano *et al.*	Tungsten	Hairpin	Electrochemical etching and annealing[10,27,28]
Velasquez-Garcia *et al.*	Silicon	Ridge	Deep reactive ion etching and SF_6 plasma etching[11,12]
Chiu *et al.*	Tungsten	Hairpin	Electropolishing and solution roughening[29]
Castro *et al.*	Tungsten	Needle	Electrochemical etching[30–32]
Perez-Martinez *et al.*	Tungsten	Hairpin	Electropolishing and solution roughening[5,6]
Guo *et al.*	Tungsten	Needle	Electrochemical etching[33]
Wright *et al.*	Tungsten	Hybrid	Electrochemical etching[34,35]

© Author(s) 2021

determined through a metallographic microscope and profilometer examination. Besides, the performance of the externally wetted ILET is verified by emission tests.

II. THE FABRICATION OF EXTERNALLY WETTED EMITTER

In this article, a simple method of fabricating an externally wetted emitter is explored whose machining accuracy can fully meet the requirements of ILET array fabrication. Besides, it is also conducive to the preliminary study of the electrospray mechanism in laboratories with a weak foundation. The complete process of fabricating an externally wetted emitter can be divided into three key stages. In the first stage, the tungsten cuboid is cut into a designed pyramid shape by LSWC. In the second stage, the cut blank is immersed in HF solution for ultrasonic cleaning. In the third stage, the emitter is electrochemically etched with DC voltage and AC voltage, including sharpening the tip and roughening the surface. In order to evaluate the removal effect of the oxide layer in the second stage, quantitative and qualitative analysis of all elements is carried out on the emitter surface before and after pickling. So as to measure the tip size and evaluate the surface wettability, the sharpened and roughened emitter is calibrated and analyzed using a metallographic microscope and profilometer, respectively. Finally, emission test is carried out. It proves that the LSWC combined with electrochemical etching could fabricate a high-quality externally wetted emitter, and the fabricating parameters are recorded by analyzing the beam current.

A. The low-speed wire cutting

The LSWC process is carried out by using an ACTSPARK CUT200P from Switzerland that is operated under FANUC systems. The working principle of LSWC is to use continuously moving brass wire as the electrode to pulse spark discharge on the workpiece. It generates high temperature above 6000 °C to remove the metal and cut the workpiece. Figure 1 shows the LSWC process to fabricate an emitter tip. The workpiece is a tungsten cuboid.

Running the CNC (Computer Numerical Control) according to a precompiled program results in a pyramid emitter as shown in Fig. 1(c). In order to improve the fabricating accuracy and the integrity of the emitter geometry, different combinations of fabrication parameters have been attempted during the LSWC process. Successfully, the combination of fabrication parameters is recorded in Table II.

B. The removal of the oxide layer by pickling

The blank is obtained according to the method shown in Fig. 1. A dense oxide layer is formed on the emitter surface due to the very high temperature at the cutting point during the LSWC process. In addition, there are pollutants from the mineral coolant that adhere to the surface of the blank. The oxide layers and pollutants increase the contact angle between the ionic liquid and the emitter surface, which can deprive the emitter of good wettability. Therefore, the oxide layer is removed by soaking the blank in 50% HF solution for about 45 min with ultrasonic cleaning. In order to investigate the

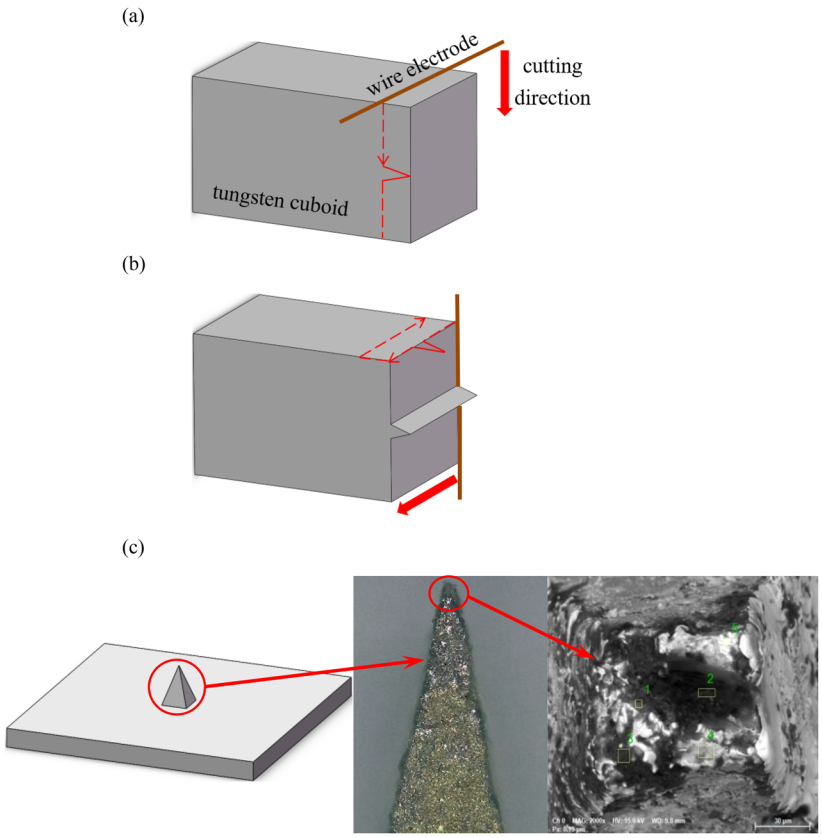

FIG. 1. LSWC process to fabricate externally wetted emitter. (a) Cutting strip. (b) Cutting pyramid. (c) Unpickled emitter and five detecting points at the tip.

© Author(s) 2021

TABLE II. The combination of fabrication parameters.

Wire material	Wire diameter	Wire tension	Wire speed	Cutting speed
Brass	0.25 mm	17 N	150 mm/s	1.14 mm/min
Coolant pressure	Coolant conductivity	Cutting power	Max. peak voltage	Max. peak current
10 pa	5 S/m	54 W	25 V	12 A

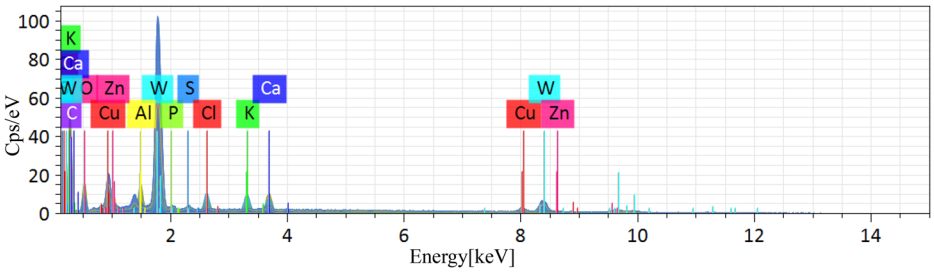

FIG. 2. SEM-EDS spectrum of unpickled emitter.

removal effect of the oxide layer, quantitative and qualitative analysis of all elements is carried out on the emitter surface before and after pickling.

Figure 2 shows all elements on the emitter surface before pickling. Analysis indicates that the tungsten cuboid itself is doped with a small amount of carbon, oxygen comes from the metallic oxide, and the rest are polluted elements. As shown in Fig. 1(c), five detection points are selected at the tip of the unpickled blank for quantitative analysis, and the results are shown in Table III.

Analyze the elements in Table III except tungsten, carbon, and oxygen. The content of cuprum is relatively high in the remaining elements. It mainly originates from the fact that the brass wire melts during the LSWC process and then adheres to the surface of the blank, as shown in Fig. 1(c). Hence, cuprum is an elementary substance. The remaining elements exist as ions that come from the coolant. According to the above-mentioned analysis, the corresponding cleaning scheme is formulated. The characteristic that tungsten is insoluble in HF solution can be used to remove the oxide layer and brass from the surface of the blank. Then, the blank is successively immersed in acetone and alcohol for ultrasonic cleaning to eliminate polluted ions.

The cleaning effect is shown in Figs. 3 and 4. The oxide layer and pollutants on the surface of the blank are removed so cleanly that the emitter can be wetted by ionic liquid. Six detection points are selected for quantitative analysis on the tip of the blank after pickling, and the results are shown in Table IV. There is little difference in the mass fraction of carbon at each detection point. The analysis shows that carbon is the impurity of the blank itself, which is also evenly distributed in the form of an elementary substance in the tungsten cuboid.

C. The electrochemical etching

A large number of scholars have studied the effects of tip radius and surface roughness on the characteristics of the ion source. For instance, Wagner reported that both the slopes of the I–V curve and the threshold voltage were increased with an increasing tip radius.[31,43] A tip with a greater radius has a greater slope of the I–V curve, whereas it requires a higher voltage, which is unfavorable to the ionic emission. Therefore, the tip radius should be designed within an appropriate range. In addition, Wagner discovered that the emitter with a smooth surface stimulated a discontinuous ionic emission mode and even a pulsed ionic emission mode while the emitter with grooves along the axial direction created a steeper I–V curve. Another scholar named Mair proved that the high flow resistance of the smooth surface reduced the thickness of the liquid metal film.[44] Mair also presented that the flow resistance was decreased as the depth of the grooves on the emitter surface increased. Thus, the increased depth and the number of axial grooves are capable

TABLE III. The quantitative analysis of unpickled emitter.

Normalized mass fraction	C	O	Al	P	S	Cl	K	Ca	Cu	Zn	W
1	17.99	10.90	0.30	0.84	1.38	5.85	6.75	5.93	6.29	1.58	42.19
2	48.51	17.81	3.29	0.00	0.94	2.19	2.06	6.93	5.30	1.03	11.94
3	11.82	6.63	1.16	0.13	0.60	1.25	0.71	9.58	17.13	3.72	47.28
4	10.68	9.75	0.15	0.42	0.75	1.00	0.63	1.83	8.04	5.69	61.08
5	8.53	7.51	0.32	0.20	0.25	0.29	0.21	1.38	7.42	0.71	73.17
Mean	19.5	10.52	1.04	0.32	0.78	2.12	2.07	5.13	8.84	2.55	47.13

© Author(s) 2021

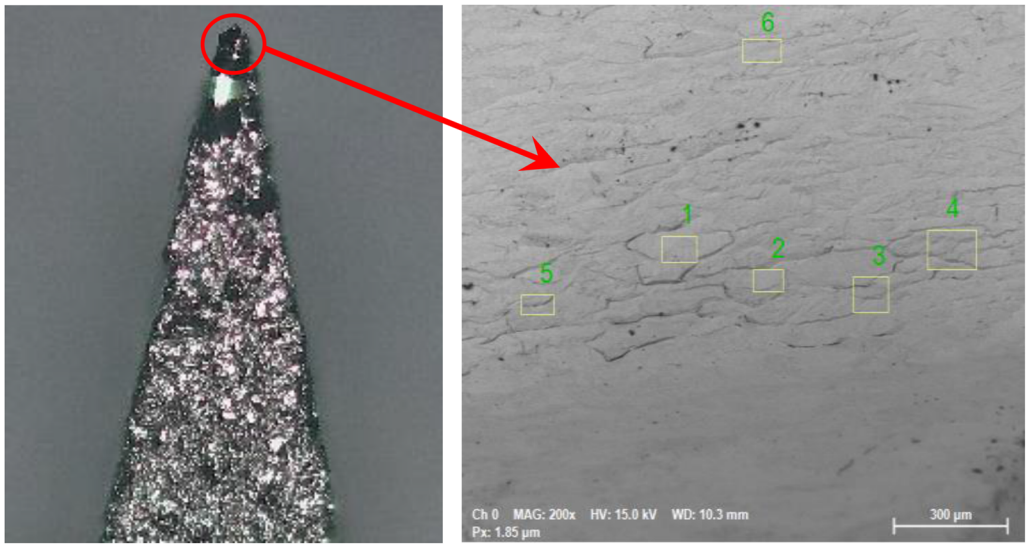

FIG. 3. (a) Pickling emitter. (b) Six detection points at the tip.

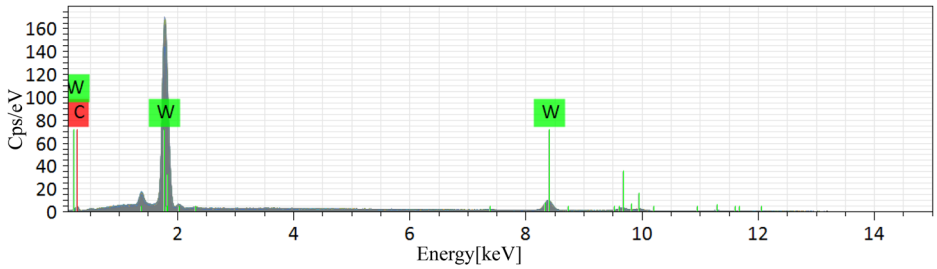

FIG. 4. SEM-EDS spectrum of pickling emitter.

of decreasing the flow resistance so as to promote continuous ionic emission.

Through the investigation of a large number of scholars' literature studies, an important conclusion can be drawn that the tip diameter of the emitter must be controlled to within 10 μm approximately if the electrospray thruster is to work efficiently and continuously in pure ionic emission mode with a low threshold of initial emission voltage. At the same time, reliable microchannels are required to maintain excellent wettability and stable flow supply on the emitter surface. Therefore, the blank in Fig. 3 is far from sufficient for emission tests. The emitter will be further fabricated by building an electrochemical etching platform as shown in Fig. 5. First and foremost, tip sharpening is implemented by electrochemical etching under DC voltage. Second, surface roughening is implemented by electrochemical etching under AC voltage. DC voltage is

TABLE IV. The quantitative analysis of pickling emitter.

Normalized mass fraction	C	W
1	3.17	96.83
2	3.42	96.58
3	3.43	96.57
4	3.70	96.30
5	3.54	96.46
6	4.16	95.85
Mean	3.57	96.43

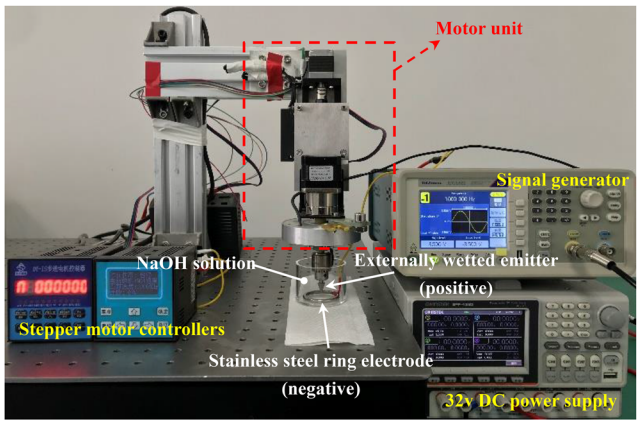

FIG. 5. Electrochemical etching platform to sharpen the tip and roughen the emitter.

© Author(s) 2021

TABLE V. The parameters of electrochemical etching for pyramid emitter. ∗ indicates the default value.

	Voltage amplitude (V)	Voltage frequency	Electrolyte concentration (mol/l)	Etching time (s)
DC voltage	3	∗	5	180
AC voltage	±3	3 Hz	5	400

provided by a 32 V DC power source, while AC voltage is generated by a signal generator. NaOH solution is used as the electrolyte, while the stainless-steel ring is used as the negative electrode, and the clamping device of the emitter is connected to the positive electrode. A motor unit is used to immerse the emitter 3 mm below the liquid level of the electrolyte and coincide with the central axis of the ring. The voltage amplitude, the frequency of AC voltage, the etching time, and the concentration of NaOH solution have a significant effect on the tip radius, microchannel width, and microchannel depth. After a lot of etching and metallographic microscope examination, the etching parameters are finally summarized as shown in Table V. It is worth noting that the etching parameters in Table V are only appropriate for the size of the pyramid emitter designed in this article. If the geometry or the scale of the emitter is changed, it will be another set of etching parameters. Consequently, the combination of 3 V and 5 mol/l can not only ensure effective electrochemical reaction but also avoid the uneven etching due to the very violent reaction. The voltage frequency is 3 Hz in order to etch the microchannel with sufficient depth and width. Finally, the tip radius is controlled by etching time; too short or too long etching time will make the tip passive. In order to obtain the ideal tip radius, the etching time should be accumulated step by step until the tip radius reaches the minimum value. Therefore, the specific etch parameters must be adjusted according to the size and material of the emitter, and the final criterion is the tip radius (<10 μm).

The sharpened and roughened externally wetted emitter is shown in Fig. 6(a) whose tip diameter is ~3 μm. The white reticular structure is a winding liquid film formed by ionic liquid wetting along the etched microchannels. As shown in Figs. 6(b) and 6(c), in order to compare the beam current characteristics with the externally wetted emitter, the same process is used to fabricate the porous tungsten emitter. However, only electrochemical etching under DC voltage is carried out to ensure that the porous structure is completely unblocked and the same tip radius is obtained. Two kinds of high-quality emitters are fabricated to meet the requirements of emission tests with unremitting attempts, which means excellent wettability and an appropriate tip radius.

The width and depth of the microchannel are important indicators to evaluate the ability of emitter transporting ionic liquid, which can be measured using a profilometer. As shown in Figs. 7 and 8, the reticular microchannels are successfully etched on the surface of the externally wetted emitter, and grooves are interconnected. A profilometer can measure the position data and height data of each pixel after scanning the surface. The width of the microchannel in 2D view and the depth of the microchannel in 3D view can be obtained by reconstructing the data. The image shows that the microchannels are uniformly distributed on the emitter surface with uniform width and depth. According to the statistics and calculation of the scanning data, the average width and the average depth of the microchannels etched on the surface of the externally wetted emitter are greater than 4 and 20 μm, respectively. By immersing the etched emitter in acetone and alcohol successively for ultrasonic cleaning, ions and WO_4^{2-} in the electrolyte can be removed. In order to improve the wettability, the dried emitter is immersed in ionic liquid for ultrasonic cleaning. The aim is to release bubbles hidden in the microchannels to fill the grooves with ionic liquid. Some scholars have confirmed that bubbles have serious adverse effects on wettability and emitting performance. As shown in Fig. 6(a), the ionic liquid wets along the emitter to the tip and forms an effective reticular liquid film, which provides a reliable flow supply for the emission tests.

Porous tungsten is sintered from pulverous tungsten under high temperature and high pressure, which is widely used in military radar. As shown in Figs. 9 and 10, pore structures with a characteristic scale of about 1 μm are evenly distributed on the surface and inside of the emitter, which can ensure sufficient ionic liquid for the ILET. The porous material has a honeycomb entity structure, which can generate greater capillary force to transport ionic liquid. Unfortunately, undersized pore structures are prone to blockage by

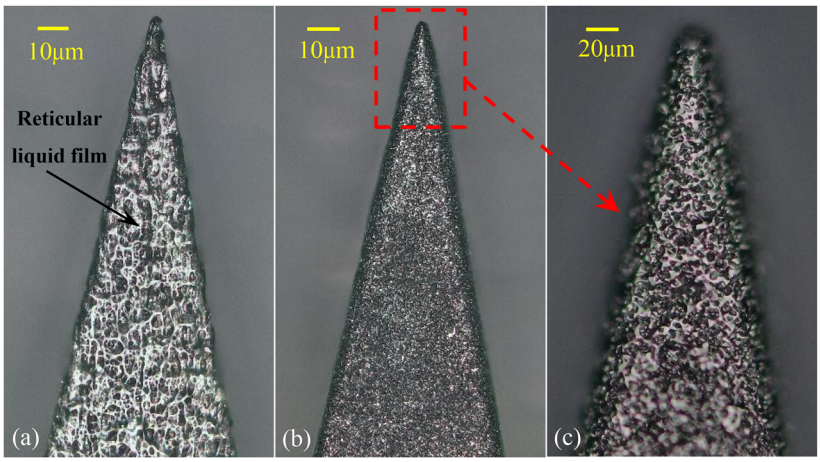

FIG. 6. Electrochemical etching emitter using parameters. (a) Externally wetted emitter after 58 h of emission. (b) Porous tungsten emitter. (c) Pore structure (~1 μm).

© Author(s) 2021

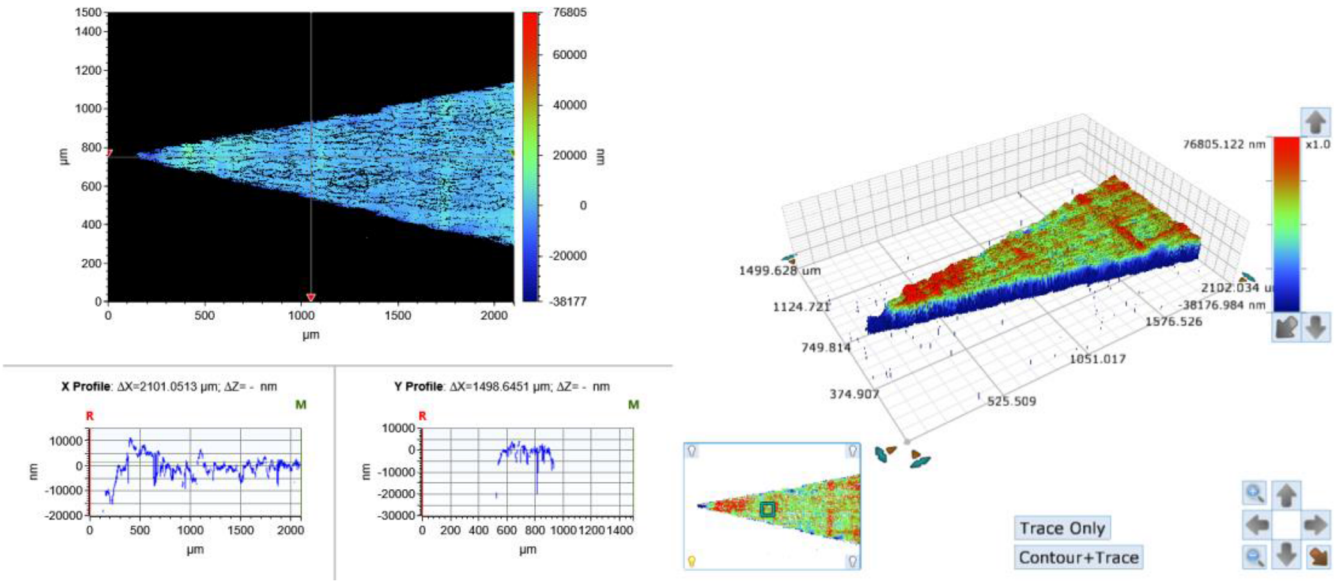

FIG. 7. Winding microchannels on the surface of externally wetted emitter.

the electrochemical reaction products after prolonged bias emission. Nevertheless, the problem of electrochemical decomposition due to extraction of single polarity ions is solved by periodically alternating the voltage source at 1 Hz so that the potential difference that appears across the double layer formed between the emitter and the liquid is maintained below the electrochemical window limit, thus eliminating electronic reactions.[28] However, due to the difference in specific charge between anions and cations and the effect of delayed emission, the effect of reaction products blocking the pore structure cannot be completely eliminated in practice.

III. THE CHARACTERISTICS OF BEAM CURRENT

As shown in Fig. 11(a), the emitter tip will not be wetted effectively by ionic liquid, and the phase interface will be the free

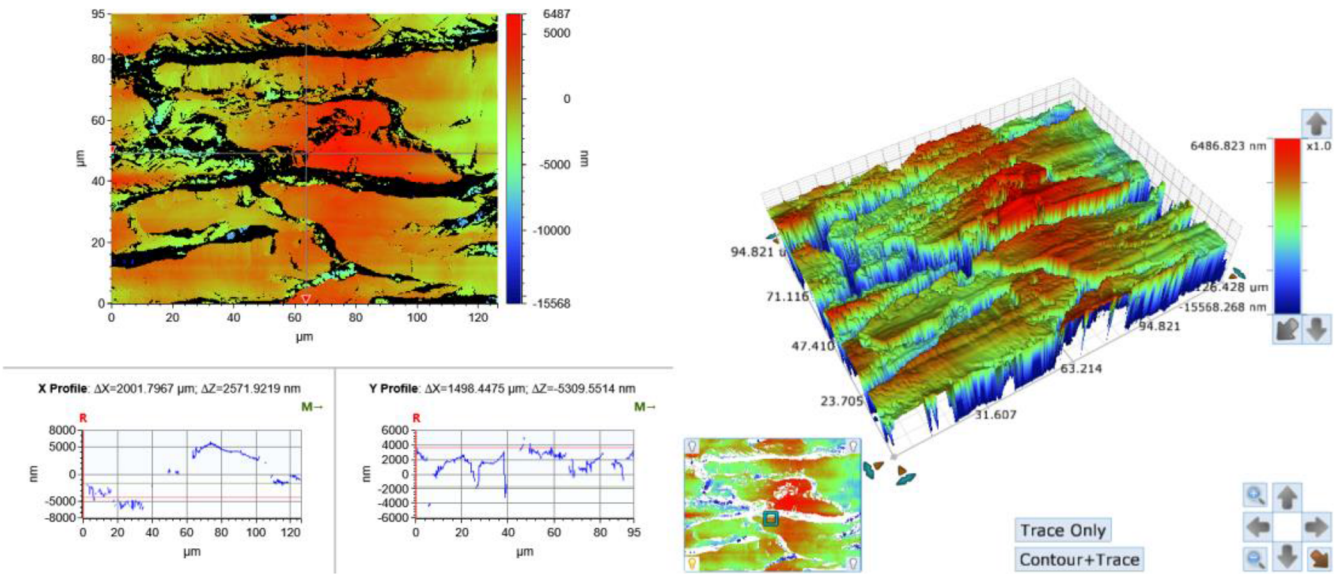

FIG. 8. Localized amplification of microchannels on the surface of externally wetted emitter.

© Author(s) 2021

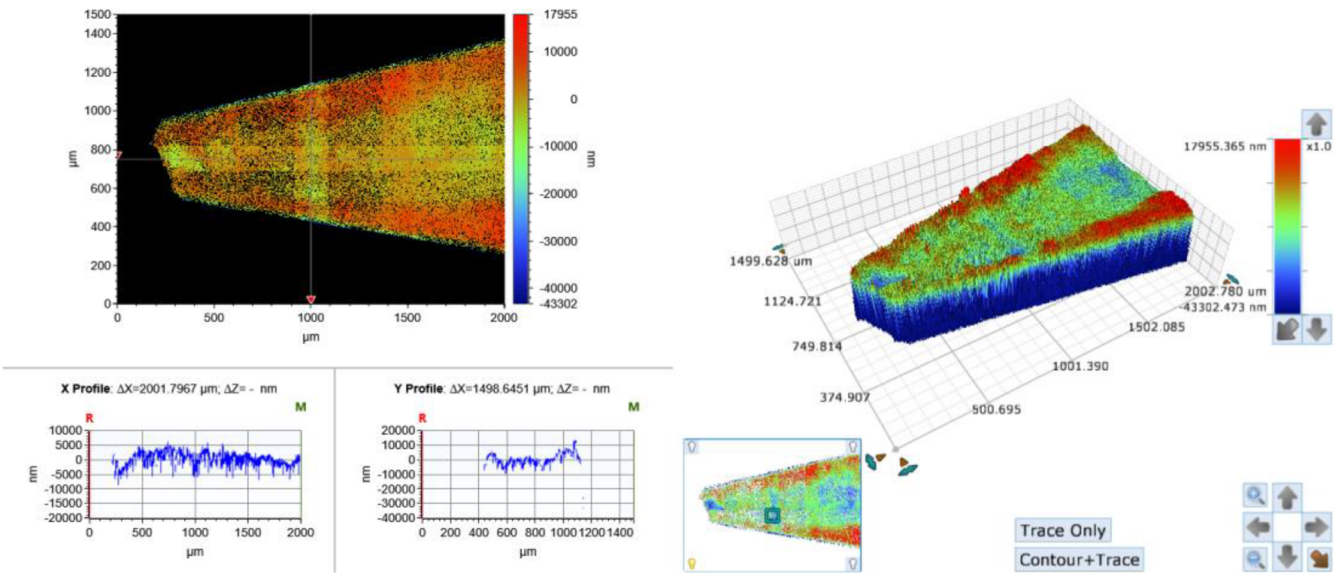

FIG. 9. Pore structure on the surface of porous tungsten emitter.

meniscus when electrostatic field is not applied. When the potential of the extractor approaches the threshold of the initial emission voltage, the ionic liquid will climb along the emitter surface to the tip by electrophoretic force. The process is called electrowetting, as shown in Fig. 11(b). As the voltage increases, the liquid at the emitter tip shrinks and deforms into a cone structure. Taylor has made a detailed study of this phenomenon.[45] The Taylor cone will be further developed into a cone jet. According to the classic Rayleigh breakage theory, the cone jet will become extremely unstable when it is disturbed by a small disturbance, and eventually, the end of the jet will break into droplets.[46–50] The thruster works in droplet emission mode with a large thrust and small specific impulse at this moment, as shown in Fig. 11(c). When the electric field intensity at the end of the jet is high enough, the charged ions or ion clusters will escape directly from the phase interface. The process is called field evaporation.[51,52] The thruster works in ionic emission mode with a large specific impulse and small thrust right now, as shown in Fig. 11(d). The study indicates that the switching of the two modes is related to the liquid flow and electric field intensity at the emitter tip.

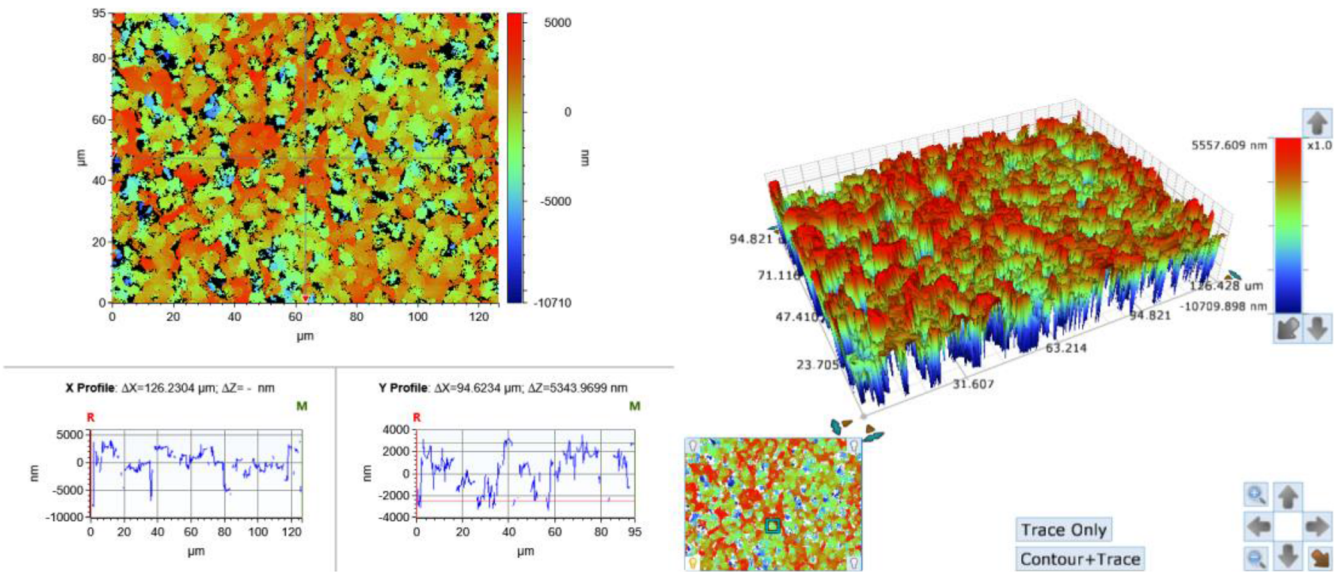

FIG. 10. Localized amplification of pore structure on the surface of porous tungsten emitter.

© Author(s) 2021

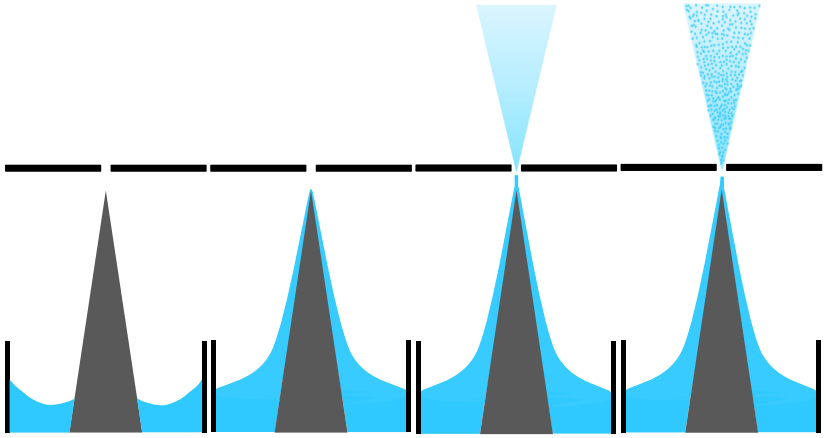

FIG.11 The electrowetting and emitting process

FIG. 11. Electrowetting and emitting process. (a) Free meniscus. (b) Electrowetting. (c) Droplet emission. (d) Ionic emission.

Recently, Lozano reported that the pure ionic emission mode could be achieved via an externally wetted needle. Hence, the ILET could be a candidate for high specific impulse missions as well.[53,54] Unlike the capillary emitter, where the flow rate control is regulated by pressure, the flow rate of an externally wetted emitter depends primarily on the wettability and tip size.[10] Besides, the externally wetted emitter facilitates the electrospray of viscous ionic liquids.

The testing system is shown in Fig. 12; in order to verify whether the externally wetted emitter fabricated in Sec. II is capable of emitting continuously and stably, emission tests are carried out. As shown in Figs. 12(b) and 12(c), the emitter is a hybrid structure that consists of a pyramid emitter and a square capillary.[42] Ions or ion clusters are ejected from the tip and fly into an electric-field-free region passing through a hole 0.6 mm in diameter drilled coaxially on the extractor. These ions or ion clusters fly at a constant speed in a vacuum chamber and impinge on a metallic collector connected to a pico-ammeter, which can capture beam current.

Definitely, the performance of the externally wetted emitter and porous tungsten emitter is investigated from the aspects of beam current resolution, the emission mode of anion and cation emitting alternately, the duration of continuous emission without flow supply, and ignition reliability. The propellant used in the emission tests is EMI-TFSI whose physical properties are shown in Table VI.

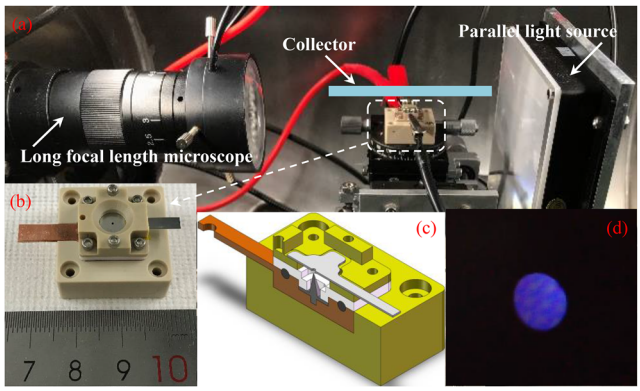

FIG. 12. Testing system to detect beam current. (a) Platform for emission tests. (b) and (c) Externally wetted ILET. (d) Plume of single emitter.

The externally wetted emitter works stably in the voltage range of 1370–1540 V within which effective and stable beam current can be obtained. When the voltage of the extractor is lower than the threshold of the initial emission voltage, the ionic liquid cannot break through the energy barrier to form effective ionic emission or droplet emission at the emitter tip. When the voltage of the extractor is higher than 1540 V, the noise of beam current will become very intense, and even intermittent electrode short circuit will occur. Similarly, the porous tungsten emitter works stably in the voltage range of 2270–2480 V. The difference in the voltage range between the two emitters is most likely due to the different electrowetting modes. Therefore, it is infeasible to compare the beam current steps of two emitters in the same voltage range.

As shown in Fig. 13, the threshold of the initial emission voltage of the externally wetted emitter is 1370 V at which cations or cation clusters are emitted. The range of effective and stable beam current is 80–110 nA, and the resolution is 1 nA. As shown in Fig. 14, the threshold of the initial emission voltage of the porous tungsten emitter is 2270 V. The range of effective and stable beam current is 144–200 nA, and the resolution is 4 nA. When the voltage increases by 20 V, the beam current of the porous tungsten emitter increases by 4 nA fixedly within the regulated range, whereas the increment in the beam current of the externally wetted emitter varies from 1 to 6 nA uniformly. The tests confirm that the beam current of the porous tungsten emitter follows the voltage well because the pore structure has a natural atomization effect on the ionic liquid vaporized in the electric field at the initial emitting moment, which is also the reason for the large initial beam current. Every pore structure at

TABLE VI. The physical properties of propellant (25 °C, 1 atm).

Abbreviation	μ (Pa s)	γ (N/m)	ρ (Kg/m^3)	ε_r (1)	σ (S/m)
EMI-TFSI	0.034	0.023 67	1520	11.3219	0.92

© Author(s) 2021

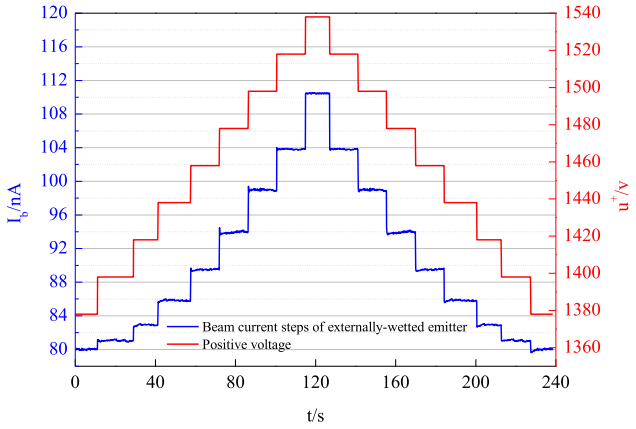

FIG. 13. Beam current range and resolution of externally wetted emitter.

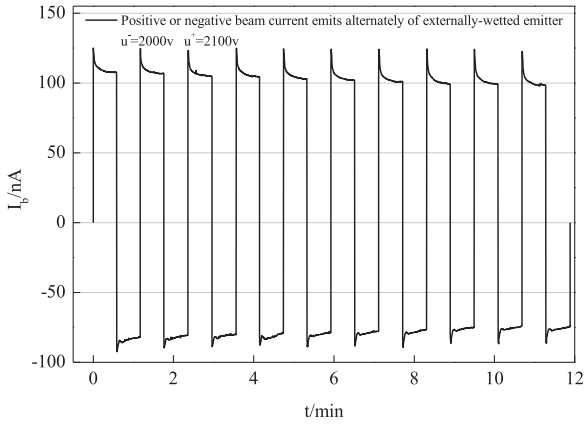

FIG. 15. Bipolar alternating emission of externally wetted emitter.

the tip of the porous tungsten emitter can be regarded as an emission point. Due to the influence of wettability, there is no guarantee that the same pore structure at the tip will be ignited each time when the same bias voltage is applied repeatedly. Hence, it is shown in Fig. 14 that the beam current cannot be leveled when the same bias voltage is applied repeatedly. On the contrary, the externally wetted emitter merely has a single microchannel for liquid supply at the tip, which makes the ionic liquid form a Taylor cone at the fixed point. At last, the Taylor cone evolved into a cone jet under the drag of a gradually stronger electrostatic force. The instability at the front end of the cone jet leads to the fragmentation of charged microdroplets. With the increase in electrostatic field, the complex ionization processes of charged microdroplets such as field evaporation and ion collision will occur. As a consequence, it is shown in Fig. 13 that the beam current can be leveled when the same bias voltage is applied repeatedly. The transition from droplet emission mode to pure ionic emission mode is also responsible for the small initial beam current of the externally wetted emitter. It can be observed from Fig. 14 that there is an obvious process of oscillating return to the stable state at the rising edge and falling edge of the beam current curve, which is called charged relaxation in the literature. The charged relaxation is mainly related to the rearrangement of charges in the double electric layer.[28,55] The fact that the externally wetted emitter has no obvious charged relaxation in this condition is beneficial for optimizing the thrust response time of the electrospray thruster. The difference in wettability leads to multi-point emission and single point emission, which is the main reason for the noise of beam current as well. Multi-point emission is more likely to generate unstable beam current intensity. By contrast, it is shown in Figs. 13 and 14 as oscillation curves with high frequency and small amplitude and horizontal curves, respectively.

To sum up, the beam current of externally wetted emitter has a narrow range. Nevertheless, the resolution of beam current is very high. Thrusters require high thrust resolution when scientific satellites perform deep space exploration missions ($\leq$0.1 μN). The beam current of the externally wetted emitter can reach a fixed value corresponding to the effective potential by repeatedly adjusting the voltage of the extractor from any potential to an effective potential. Excellent reproducibility makes the externally wetted emitter a more reliable and convenient control system.

There is an important issue concerning the operation of electrosprays in the purely ionic regime, that is, the fate of counterions that are left behind in the liquid when a single polarity is extracted.

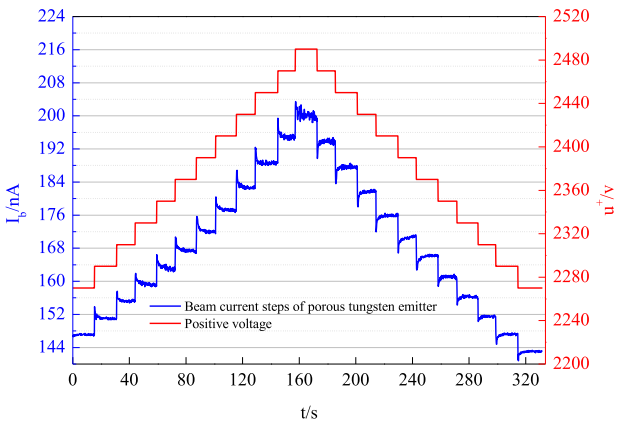

FIG. 14. Beam current range and resolution of porous tungsten emitter.

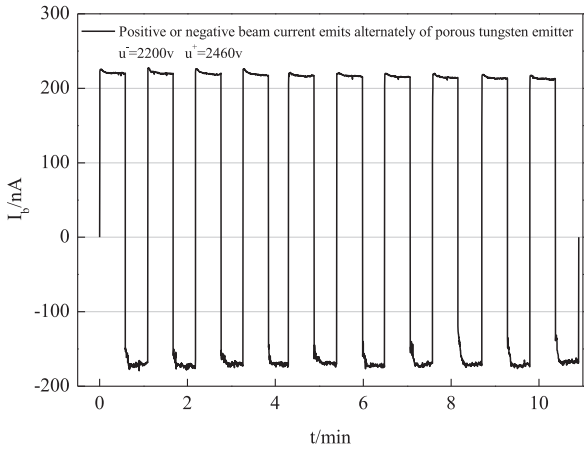

FIG. 16. Bipolar alternating emission of porous tungsten emitter.

© Author(s) 2021

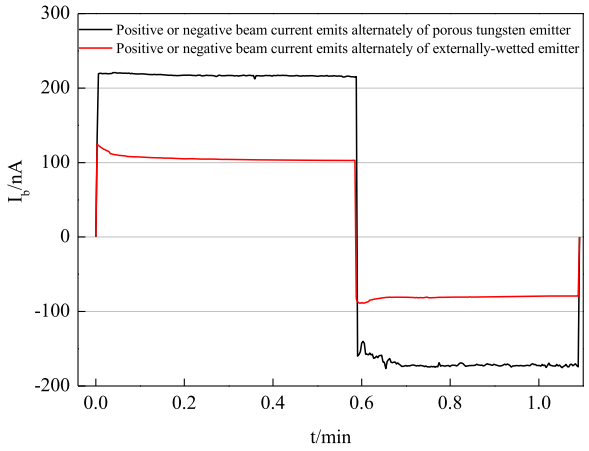

FIG. 17. Localized amplification of Figs. 15 and 16.

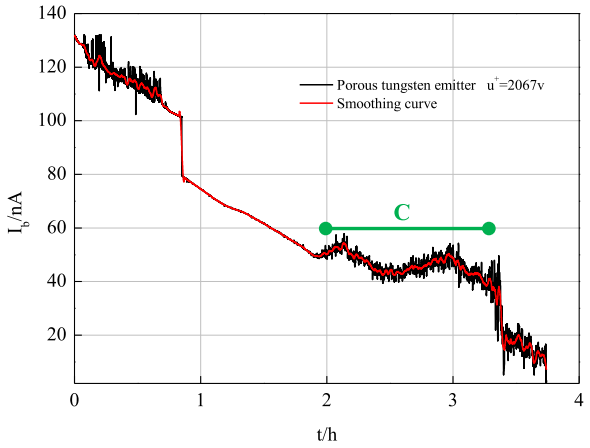

FIG. 19. Continuous emission of porous tungsten emitter without flow supply.

It is likely that in solvent-based electrosprays, most of these counterions and/or their reaction products leave the solution along with emitted liquid droplets in a "self-cleaning" mode, producing little degradation. In the case of purely ionic liquid, these counterions definitely stay behind to eventually interact electrochemically with the remaining liquid, the electrode, or both. The outcome of such interaction, always detrimental to the thrust performance, determines the applicability of the ILET as a reliable device. It will be shown that electrochemical reactions can be avoided by using polarity alternation at a frequency dictated by the magnitude of the electrochemical window of the ionic liquid.[28]

Ion emission from the ILET is successfully achieved without electrochemical reactions. This is accomplished by alternating the voltage of the power supply at a minimum frequency determined by the charging time of the double layer that appears across the liquid–metal interface to a voltage lower than the electrochemical window. As shown in Figs. 15 and 16, the bipolar alternating emission can be achieved by both types of emitters. The purpose is to eliminate the pollutants generated by the electrochemical reaction between the emitter and the ionic liquid during the emitting process, which will block the microchannel and pore structure, leading to the thruster failure. Meanwhile, the bipolar alternating emission at an appropriate frequency can also achieve the aim of self-neutralizing the positive charges and negative charges on the surface of the spacecraft, which reduces the dependence on the neutralizer. As shown in Fig. 17, neither the externally wettable emitter nor the porous tungsten emitter can accurately maintain positive beam current and negative beam current equally. It means that there will be redundancy of positive charges after each polarity conversion cycle. There are great possibilities that the different specific charges of anions and cations lead to different electrochemical windows. The frequency of voltage polarity alternation depends on the charging time of the double electric layer that appears across the liquid–metal interface.[28] As shown in Fig. 16, the noise of negative beam current is always greater than that of positive beam current. It may be that the pore structures produce a relatively larger area of the double electric layer. This in turn maximizes the net capacitance and therefore the charging time. Therefore, the frequency of voltage polarity alternation fixed in the tests is only conducive to the stability of the positive emission.

The fatigue tests of the ILET without flow supply are arranged to evaluate the capability of continuous emission and to assess the damage status of critical components. The two types of emitters

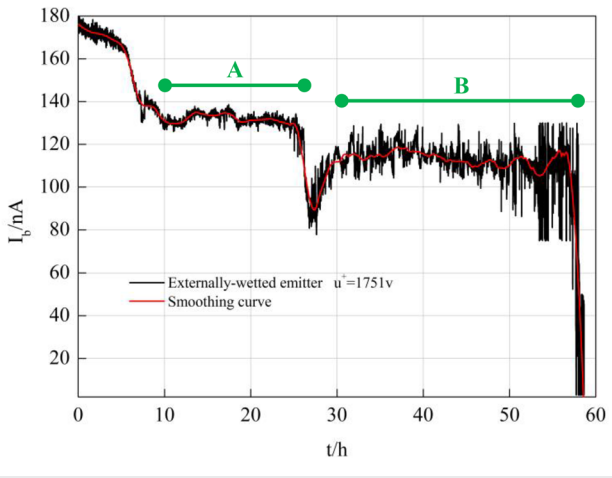

FIG. 18. Continuous emission of externally wetted emitter without flow supply.

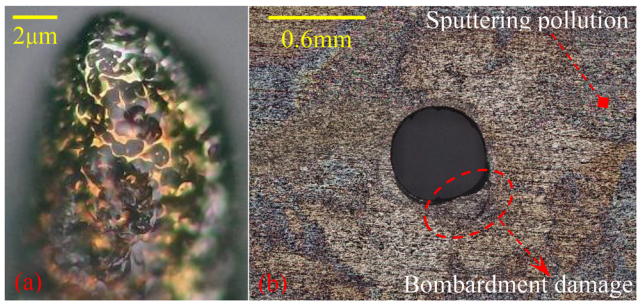

FIG. 20. (a) Pore structures are blocked by electrochemical products. (b) Extractor damage after 3.7 h emission.

© Author(s) 2021

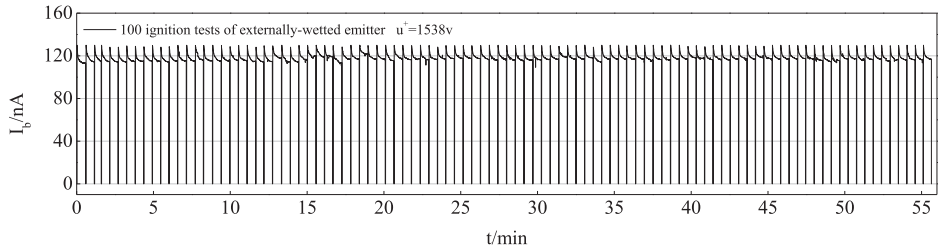

FIG. 21. Ignition testing of externally wetted emitter.

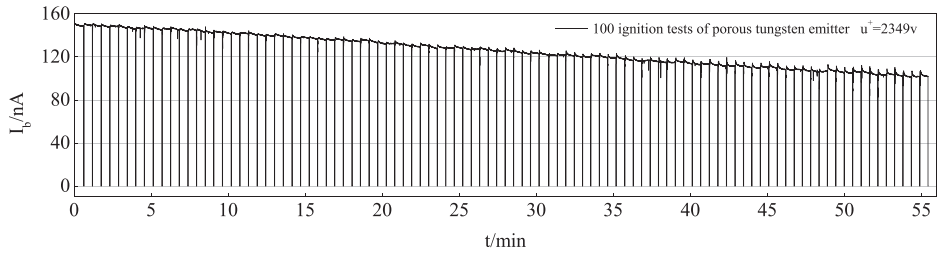

FIG. 22. Ignition testing of porous tungsten emitter.

mainly rely on the meniscus formed by the hybrid structure to maintain wetness during the testing.[42] As shown in Fig. 18, the externally wetted emitter has a total duration of 58 h of continuous emission including the stable emission of segment A (17 h 130 nA) and segment B (27 h 110 nA). The ionic liquid reserve in segment A is relatively more abundant so that the noise of beam current is lower. The externally wetted emitter after 58 h of fatigue tests is shown in Fig. 6(a), which still possesses characteristics of excellent wettability and integrity. Besides, the microchannels are still unobstructed as expected. It is observed that the ionic liquid has almost been consumed by the thruster during the dismantling process. Consequently, the externally wetted emitter stops emitting because of no additional propellant supply. As shown in Fig. 19, the beam current of the porous tungsten emitter continues to decay within 3.8 h, including the stable emission in segment C (1.3 h 40nA–50 nA). As shown in Fig. 20(a), the yellow colloidal substance is found attached to the surface of the porous tungsten emitter. Furthermore, it is observed that the ionic liquid has not been completely consumed by the thruster during the dismantling process. In summary, the porous tungsten emitter stops emitting because the pore structure is blocked by the reaction products. As shown in Fig. 20(b), there is serious pollution and damage caused by sputtering and ion bombardment, respectively, around the hole of the extractor. In reality, the injury could be effectively avoided by increasing the transmittance and decreasing the plume angle.

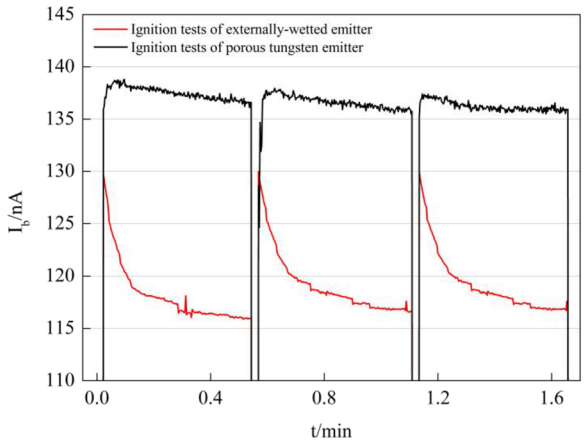

FIG. 23. Localized amplification of Figs. 21 and 22.

In conclusion, the externally wetted emitter performs well in fatigue tests because it not only has a long emission life but also has lower noise of beam current when the emitter is wetted sufficiently. The hybrid externally wetted emitter will show great potential in fatigue testing if equipped with a continuous and stable propellant supply system.

As shown in Figs. 21 and 22, the results of ignition tests indicate that the ignition success rates of both emitters are 100%. The beam current of the porous tungsten emitter decreases with the increase in ignition times. In contrast, the beam current of the externally wetted emitter remains constant, showing repeatability as shown in Fig. 13. As shown in Fig. 23, the beam current curve of the porous tungsten emitter shows an oscillation with small amplitude and high frequency at the moment of successful ignition, which is consistent with the previous testing results.

IV. CONCLUSION

The article explores a new technology that is a combination of low-speed wire cutting (LSWC) with electrochemical etching to fabricate the externally wetted emitter. The fabrication parameters have been recorded by observing and testing repeatedly, including the frequency of etching voltage, the etching time, the concentration of electrolyte, and the depth of emitter immersion in solution. The externally wetted emitter fabricated by the above-mentioned technology possesses excellent wettability to achieve continuous and stable flow supply. Compared with the porous tungsten emitter, the microchannels etched on the surface of the externally wetted emitter are not easily blocked by reaction products. In addition, the ILET equipped with only a biased power source is competent for space missions that require a thruster to emit efficiently for a long time. The emission tests demonstrate that the beam current of the

© Author(s) 2021

externally wetted emitter has lower noise, higher resolution, and better repeatability. As a consequence, it is proved that the technology described in this article can fully satisfy the requirements of fabricating the emitter.

ACKNOWLEDGMENTS

This work was supported by the Strategic Priority Research Program of the Chinese Academy of Science (Grant No. XDB23030300) and the National Natural Science Foundation of China (Grant Nos. 12032020 and 12072354).

AUTHOR DECLARATIONS

Conflict of Interest

The authors have no conflicts to disclose.

DATA AVAILABILITY

The data that support the findings of this study are available from the corresponding author upon reasonable request.

REFERENCES

[1]P. Prewett and G. Mair, *Focused Ion Beams from Liquid Metal Ion Sources* (Research Studies Press Wiley, 1991).
[2]C. Bartoli, H. V. Rohden, S. P. Thompson *et al.*, "A liquid caesium field ion source for space propulsion," J. Phys. D: Appl. Phys. **17**(12), 2473 (2000).
[3]W. Steiger, A. Genovese, and M. Tajmar, "Micronewton indium FEEP thrusters," The 3rd International Conference on Spacecraft Propulsion, 2000.
[4]D. Krejci, F. Mier-Hicks, R. Thomas *et al.*, "Emission characteristics of passively fed electrospray microthrusters with propellant reservoirs," J. Spacecr. Rockets **54**(2), 447 (2017).
[5]C. Perez-Martinez *et al.*, "Ionic liquid ion sources as a unique and versatile option in FIB applications," Microelectron. Eng. **88**(8), 2088–2091 (2011).
[6]C. Perez-Martinez, S. Guilet, N. Gogneau *et al.*, "Development of ion sources from ionic liquids for microfabrication," J. Vac. Sci. Technol. B **28**(3), L25–L27 (2010).
[7]M. Takeuchi, "Development of ionic liquid ion source with porous emitter for surface modification," Nucl. Instrum. Methods Phys. Res., Sect. B **315**, 345 (2013).
[8]M. Wortmann, A. Ludwig, J. Meijer *et al.*, "High-resolution mass spectrometer for liquid metal ion sources," Rev. Sci. Instrum. **84**(9), 093305 (2013).
[9]Y. Nan, *Focused Ion Beam Systems: Basics and Applications* (Cambridge University Press, 2007).
[10]P. Lozano and M. Martínez-Sánchez, "Ionic liquid ion sources: Characterization of externally wetted emitters," J. Colloid Interface Sci. **282**(2), 415–421 (2005).
[11]L. F. Velasquez-Garcia, A. I. Akinwande, and M. Martinez-Sanchez, "A planar array of micro-fabricated electrospray emitters for thruster applications," J. Microelectromech. Syst. **15**, 1272–1280 (2006).
[12]B. Gassend, L. F. Velasquez-Garcia, A. I. Akinwande *et al.*, "A microfabricated planar electrospray array ionic liquid ion source with integrated extractor," J. Microelectromech. Syst. **18**(3), 679–694 (2009).
[13]D. Garoz, C. Bueno, C. Larriba *et al.*, "Taylor cones of ionic liquids from capillary tubes as sources of pure ions: The role of surface tension and electrical conductivity," J. Appl. Phys. **102**(6), 064913 (2007).
[14]R.Krpoun and H. R. Shea, "Integrated out-of-plane nanoelectrospray thruster arrays for spacecraft propulsion," J. Micromech. Microeng. **19**(4), 045019 (2009).
[15]S. Dandavino *et al.*, "Microfabricated electrospray emitter arrays with integrated extractor and accelerator electrodes for the propulsion of small spacecraft," J. Micromech. Microeng. **24**(7), 075011 (2014).
[16]T. Henning, K. Huhn, L. W. Isberner, and P. J. Klar, "Miniaturized electrospray thrusters," IEEE Trans. Plasma Sci. **46**, 214–218 (2018).
[17]R. S. Legge and P. C. Lozano, "Electrospray propulsion based on emitters microfabricated in porous metals," J. Propul. Power **27**(2), 485–495 (2015).
[18]D. G. Courtney, H. Li, and P. C. Lozano, "Electrochemical micromachining on porous nickel for arrays of electrospray ion emitters," J. Microelectromech. Syst. **22**(2), 471–482 (2013).
[19]C. S. Coffman and P. C. Lozano, "On the manufacturing and emission characteristics of dielectric electrospray sources," in AIAA/ASME/SAE/ASEE Joint Propulsion Conference, 2013.
[20]C. S. Perez-Martinez and P. C. Lozano, "Ion field-evaporation from ionic liquids infusing carbon xerogel microtips," Appl. Phys. Lett. **107**(4), 043501 (2015).
[21]D. G. Courtney, H. Shea *et al.*, "Comparing direct and indirect thrust measurements from passively fed ionic electrospray thrusters," J. Propul. Power **32**(2), 392–407 (2016).
[22]J. Rojas-Herrera, I. Jivanescu, D. Freeman *et al.*, "Porous materials for ion-electrospray spacecraft microengines," J. Nanomech. Micromech. **7**(3), 04017006 (2017).
[23]J. Ziemer, M. Gamero-Castaño, V. Hruby *et al.*, "Colloid micro-Newton thruster development for the ST7-DRS and LISA missions," in AIAA/ASME/SAE/ASEE Joint Propulsion Conference & Exhibit, 2005.
[24]N. R. Demmons, D. Courtney, N. Alvarez *et al.*, "Component-level development and testing of a colloid micro-thruster (CMT) system for the LISA mission," in AIAA Propulsion and Energy 2019 Forum, 2019.
[25]M. Gamero-Castaño, R. E. Wirz *et al.*, "LISA colloid microthruster technology development plan and progress," in International Electric Propulsion Conference, 2019.
[26]J. Ziemer, C. Marrese-Reading, C. Dunn *et al.*, "Colloid microthruster flight performance results from space technology 7 disturbance reduction system," in 35th International Electric Propulsion Conference, Atlanta, GA, 2017.
[27]P. Lozano, M. Martinez-Sanchez, and J. M. Lopez-Urdiales, "Externally wetted ionic liquid thruster," in 4th International Spacecraft Propulsion Conference, 2004.
[28]P. Lozano and M. Martínez-Sánchez, "Ionic liquid ion sources: Suppression of electrochemical reactions using voltage alternation," J. Colloid Interface Sci. **280**(1), 149–154 (2004).
[29]Y. Chiu, G. Gaeta, T. R. Heine *et al.*, "Analysis of the electrospray plume from the EMI-Im propellant externally wetted on a tungsten needle," in AIAA/ASME/SAE/ASEE Joint Propulsion Conference and Exhibit (2006).
[30]S. Castro and J. Fernández de la Mora, "Effect of tip curvature on ionic emissions from Taylor cones of ionic liquids from externally wetted tungsten tips," J. Appl. Phys. **105**(3), 034903 (2009).
[31]A. Wagner and T. M. Hall, "Liquid gold ion source," J. Vac. Sci. Technol. **16**(6), 1871–1874 (1979).
[32]W. Driesel, "Low-energy ion optical system with a liquid-metal ion source for imaging and processing solid structures," Ultramicroscopy **52**(1), 65–72 (1993).
[33]D. Guo, X. Kang, J. Hu *et al.*, "Note: Fabrication of roughened tips for liquid metal ion sources," Rev. Sci. Instrum. **88**(6), 066107 (2017).
[34]P. L. Wright, H. Huh, N. M. Uchizono *et al.*, "A novel variable mode emitter for electrospray thrusters," in International Electric Propulsion Conference, 2019.
[35]J. Brady, "A simple technique for making very fine, durable dissecting needles by sharpening tungsten wire electrolytically," Bull. World Health Organ. **32**(1), 143–144 (1965).
[36]A. I. Oliva *et al.*, "Electrochemical preparation of tungsten tips for a scanning tunneling microscope," Rev. Sci. Instrum. **67**(5), 1917–1921 (1996).
[37]J. P. Song, N. H. Pryds *et al.*, "A development in the preparation of sharp scanning tunneling microscopy tips," Rev. Sci. Instrum. **64**(4), 900–903 (1993).
[38]M. Cavallini and F. Biscarini, "Electrochemically etched nickel tips for spin polarized scanning tunneling microscopy," Rev. Sci. Instrum. **71**(12), 4457–4460 (2000).
[39]L. A. Nagahara, T. Thundat, and S. M. Lindsay, "Preparation and characterization of STM tips for electrochemical studies," Rev. Sci. Instrum. **60**(10), 3128–3130 (1989).
[40]L. Anwei, H. Xiaotang, L. Wenhui *et al.*, "An improved control technique for the electrochemical fabrication of scanning tunneling microscopy microtips," Rev. Sci. Instrum. **68**(10), 3811–3813 (1997).

© Author(s) 2021

[41]X. Liu, W. He, X. Kang *et al.*, "Fabrication of porous emitters for ionic liquid ion source by wire electrical discharge machining combined with electrochemical etching," Rev. Sci. Instrum. **90**(12), 123304 (2019).
[42]S. Xue, L. Duan, and Q. Kang, "Study on the emitter infiltration of needle-capillary ionic liquid electrospray thruster," AIP Adv. **11**(3), 035234 (2021).
[43]A. Wagner, "The hydrodynamics of liquid metal ion sources," Appl. Phys. Lett. **40**(5), 440–442 (1982).
[44]G. L. R. Mair, "The effects of flow impedance on the current-voltage characteristics of liquid-metal ion sources," J. Phys. D: Appl. Phys. **30**(13), 1945 (1997).
[45]G. I. Taylor, "Disintegration of water drops in an electric field," Proc. R. Soc. London, Ser. A **280**(1382), 383–397 (1964).
[46]J. Mora and I. G. Loscertales, "The current emitted by highly conducting Taylor cones," J. Fluid Mech. **260**, 155 (2006).
[47]W. V. Hoeve, S. Gekle, J. H. Snoeijer *et al.*, "Breakup of diminutive Rayleigh jets," Phys. Fluids **22**(12), 122003 (2010).
[48]J. M. López-Herrera, A. M. Gañán-Calvo, S. Popinet *et al.*, "Electrokinetic effects in the breakup of electrified jets: A volume-of-fluid numerical study," Int. J. Multiphase Flow **71**, 14–22 (2015).
[49]M. Cloupeau and B. Prunet-Foch, "Electrostatic spraying of liquids in cone-jet mode," J. Electrost. **22**(2), 135–159 (1989).
[50]I. Marginean, P. Nemes, L. Parvin *et al.*, "How much charge is there on a pulsating Taylor cone?," Appl. Phys. Lett. **89**(6), 064104 (2006).
[51]I. Romero-Sanz, R. Bocanegra, J. Fernandez de la Mora *et al.*, "Source of heavy molecular ions based on Taylor cones of ionic liquids operating in the pure ion evaporation regime," J. Appl. Phys. **94**(5), 3599–3605 (2003).
[52]J. V. Iribarne, "On the evaporation of small ions from charged droplets," J. Chem. Phys. **64**(6), 2287–2294 (1976).
[53]P. C. Lozano, "Energy properties of an EMI-Im ionic liquid ion source," J. Phys. D: Appl. Phys. **39**(1), 126 (2005).
[54]Y. H. Chiu, B. L. Austin, R. A. Dressler *et al.*, "Mass spectrometric analysis of colloid thruster ionic emission from selected propellants," J. Propul. Power **21**(3), 416 (2012).
[55]X. Jiang, Y. Liu, and R. Qiao, "Current rectification for transport of room-temperature ionic liquids through conical nanopores," J. Phys. Chem. C **120**(8), 4629–4637 (2016).

© Author(s) 2021